Mechanics of Composite Materials, Vol. 44, No. 5, 2008

ESTIMATION OF LAMINATE STIFFNESS REDUCTION DUE TO CRACKING OF A TRANSVERSE PLY BY EMPLOYING CRACK INITIATION- AND PROPAGATION-BASED MASTER CURVES

J. Andersons,* E. Spārniņš,*
O. Rubenis,* and R. Joffe**

Keywords*: polymer-matrix composite, laminate, intralaminar cracking, stiffness*

The applicability range of toughness- and strength-based criteria for progressive cracking of a transverse layer in a cross-ply composite laminate subjected to tensile loading is considered. Using a deterministic cracking model, approximate relations for the crack density as a function of stress are derived for initiation- and propagation-controlled types of cracking. The master-curve approach is applied to progressive cracking in glass/epoxy laminates. The accuracy of estimation of laminate stiffness reduction by using crack density master curves is evaluated.

1. Introduction

The elaboration of a model for initial damage accumulation, i.e., for cross-ply cracking, in laminated composites has attracted considerable research effort, as exemplified by reviews [1-4]. The presence of transverse cracks as such is usually not critical to the load-bearing capacity and structural integrity of the composites, the principal concern being the stiffness reduction associated with cracking. A number of models relating the stiffness characteristics of a fiber-reinforced composite to the crack density (CD) in its plies have been created [5, 6]. However, in order to evaluate the stiffness reduction upon given loading, the corresponding CD has to be determined.

The cracking of a transverse ply in a composite laminate subjected to tensile loading has been first considered in a systematic manner in the 1970s [7-10] based on glass-fiber-reinforced composites. It was shown that the progressive cracking could be described by using a strength criterion for the repetitive failure of a transverse ply [7, 10, 11]. Contrarily, the strength criterion complied with the crack onset strain (COS) only for a relatively thick transverse ply, failing to predict the pronounced thickness dependence of COS for thin transverse plies accurately captured by the energy release rate ERR-based criterion of cracking [9]. The mentioned transition from the ERR-controlled to the strength-controlled cracking at a certain thickness of the transverse ply has been observed for both glass- and carbon-fiber-reinforced cross-ply composites [9, 12-14].

---

*Institute of Polymer Mechanics, University of Latvia, 23 Aizkraukles St., LV-1006, Riga, Latvia. **Division of Polymer Engineering, Luleå University of Technology, SE-971 87 Luleå, Sweden. Russian translation published in Mekhanika Kompozitnykh Materialov, Vol. 44, No. 5, pp. 633-646, September-October, 2008. Original article submitted March 17, 2008.

As origins of transverse cracks, such imperfections of ply structure as voids and regions of high fiber density were identified [7]. The imperfections are thought to facilitate fiber debonding, leading to the appearance of microcracks [15]. The growth conditions for such flaws, modeled as elliptical cracks in an anisotropic homogeneous ply, were considered in [12]. An analysis of ERRs available for the thicknesswise and widthwise propagation of microcracks allowed the authors to distinguish two different cracking scenarios, corresponding to thin and thick transverse plies.

A ply is considered thin if the flaws present span the whole its thickness. Then only the widthwise propagation condition has to be established. As the cracks of such a size are typically of a steady-state length, they start growing as soon as the steady-state ERR reaches the critical ERR, G_{ss} G_c, i.e., the fracture mechanics criterion of cracking prevails. The steady-state ERR, G_{ss}, can be accurately determined by employing, e.g., a finite fracture mechanics analysis [1].

A ply is considered thick if its thickness considerably exceeds the characteristic flaw size. In this case, the microcracks first propagate in the thickness direction, at a critical stress practically independent of ply thickness, and then, at the same load level, they also span the width of the ply [12]. Thus, the cracking onset in a thick ply is controlled by the critical stress. The latter is either close to or slightly exceeds the transverse tensile strength of a UD composite [9, 12-14].

A detailed analysis of initiation and propagation conditions of transverse cracks has been performed in [16, 17]. Extensive experimental studies of cracking in CFRP cross-ply specimens with a range of thickness of the transverse ply and either polished or notched edges are reported in [16]. The crack development in GFRP cross-ply laminates, with two different thicknesses of the transverse ply, under off-axis tension is analyzed in [17]. The analyses strongly suggest that the ply strain (or equivalently, the transverse stress in the ply) controls the initiation of transverse cracks, whereas the ERR governs the crack propagation.

Both the initiation and the propagation criteria have to be fulfilled for a crack to appear at a given load. The schematic of the dependence of COS on the thickness of the transverse ply shown in Fig. 1 illustrates the interplay of strength and critical ERR criteria [13, 18] (see the discussion in [14]). For thicker plies, the initiation criterion determines the onset of cracking, because the ERR criterion is met already at lower loads. Conversely, for thin transverse plies, a crack is stable upon its initiation, and the load has to be increased to meet the propagation criterion. The same sequence of initiation and propagation events applies not only to crack onset, but also to progressive cracking [14]. It should be noted that, should the laminate sustain a damage leading to through-the-thickness flaws, it is the propagation criterion that governs the onset of a transverse crack, regardless of ply thickness [12].

In this paper, we derive relations of master curves for initiation-controlled and propagation-controlled cracking, assuming a deterministic strength and a deterministic critical ERR, respectively, apply them to a progressive cracking analysis of glass/epoxy cross-ply laminates with different structures, and also evaluate the accuracy of the master-curve approach to predicting the composite stiffness reduction due to cracking.

2. Deriving the Master Curves of Progressive Cracking

2.1. Initiation-controlled cracking. Consider the in-plane tensile loading of a cross-ply composite laminate of structure $[0_n/90_m]_s$ by a stress $_c$ normal to the reinforcement direction of the transverse ply. The in-plane stress $_0$ in an intact transverse unidirectionally reinforced (UD) ply is estimated as

$$_0 \quad {}^{r}_{2} \quad \frac{E_2}{E_{c0}} \quad _c, \tag{1}$$

where ${}^{r}_{2}$ is the residual stress in the transverse ply, E_2 stands for the transverse modulus of the UD composite, and E_{c0} is Young's modulus of the cross-ply composite in the loading direction. The appearance of cracks causes a nonuniform stress distribution in the plies. The variation of stress in the transverse ply between two adjacent cracks spaced at a distance L can be estimated by the shear-lag model as [3]

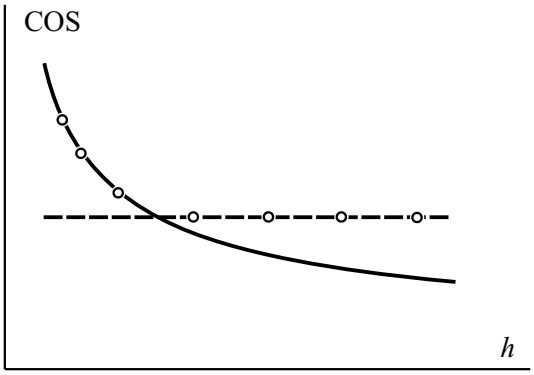

Fig. 1. Schematic of the onset of initiation- and propagation-controlled cracking in a cross-ply composite; h is the thickness of the transverse ply. O — typical experimental results; (——) — ERR-based criterion; (- - -) — strength criterion.

$$(x) \quad {}_0 \; 1 \; \frac{\cosh \; (x \;\; L/2)}{\cosh \;\; L/2} \;\; , \tag{2}$$

where is the shear-lag parameter (the inverse of the stress transfer length) and the origin of the x axis coincides with one of the cracks.

For a deterministic ply strength, a new crack should appear at the spot of highest stresses, i.e., midway between the existing cracks, as soon as the stress $(L/2)$ reaches the critical level. As the strength criterion governs the initiation-controlled cracking, we designate the critical stress by ${}_{\text{init}}$; hence, the condition for cracking becomes $(L/2) = {}_{\text{init}}$. Using Eq. (2), the cracking criterion can be transformed to

$$\frac{{}_0}{{}_{\text{init}}} \quad 1 \quad \frac{1}{2\sinh^2 \;\; L/4}. \tag{3}$$

At an advanced cracking stage, the crack spacing becomes smaller than the stress transfer length, $L \quad 1$. Expanding the denominator in the rhs of Eq. (3) in power series of L and retaining only the first term, we obtain

$$\frac{{}_0}{{}_{\text{init}}} \quad 1 \quad \frac{8}{(\;\; L)^2}. \tag{4}$$

The deterministic models of progressive cracking typically follow the scenario of a regular crack arrangement, starting, e.g., with the first crack at the specimen center, the next two cracks at specimen ends, and assuming that each subsequent crack generation is formed midway between the existing cracks [10, 11]. Thus, the crack density is related to the crack spacing as $/L$, and Eq. (4) can be rearranged in the form

$$- \quad {}^2 \qquad C_{\text{init}} \; \frac{{}_0}{{}_{\text{init}}} \quad 1 \tag{5}$$

with the factor C_{init} equal to 1/8.

Interpreting Eq. (5) as a continuous relation between the ply stress and CD in the ply, we obtain the master curve of initiation-controlled cracking, valid for an advanced cracking stage, i.e., for interacting cracks. Note that the same functional form of the master curve has been proposed in [14] based on a probabilistic cracking model [19].

2.2. Propagation-controlled cracking The ERR as a function of location between two preexisting cracks spaced at a distance L has been derived in [20]:

$$G(x) \quad G_0 \ \tanh \frac{x}{2} \quad \tanh \frac{(L \quad x)}{2} \quad \tanh \frac{L}{2} \quad , \tag{6}$$

where G_0 stands for the far-field ERR (i.e., the ERR available in an intact transverse ply). The maximum of ERR is reached midway between the cracks, therefore, a new crack appears there as soon as the propagation criterion, $G(L/2) \quad G_c$, is met. The cracking criterion can be easily expressed via the ply stress and the critical stress for crack propagation, $\quad_{prop}$. Note that the far-field ERR in the transverse ply is related to the stress as $G_0 \sim \ ^2_0$; the same holds true for the critical ERR and $\quad_{prop}$, therefore $G_0 / G_c \quad (\ _0 / \ _{prop})^2$. With account of this fact and Eq. (6), the condition for appearance of a crack midway the spacing L becomes

$$\frac{\ _0}{\ _{prop}} \quad 1 \Big/ \sqrt{2 \tanh \frac{L}{4} \quad \tanh \frac{L}{2}} \ . \tag{7}$$

Expanding the denominator in the rhs of Eq. (7) in power series of $\ L$ up to the first term and rearranging the expression as above, we finally obtain

$$- \quad ^{3/2} \qquad C_{prop} \ \frac{\ _0}{\ _{prop}} \quad 1 \tag{8}$$

with the factor C_{prop} equal to $1/4\sqrt{2}$. Equation (8) can be interpreted as a master curve for the propagation-controlled cracking; the same relation for the master curve has been obtained in [14] by a different procedure.

3. Results

3.1. Master-curve parameters . The relations for initiation- and propagation-controlled cracking, Eqs. (5) and (8), comprise such material- and lay-up-dependent characteristics as the crack onset and propagation stresses and the shear-lag parameter of the cross-ply laminate, as well as the material-independent prefactors. C_{init} and C_{prop} were evaluated in [14] by fitting the theoretical master curves to test data. The shear-lag parameter $\quad$ employed in [14] was obtained as [21]

$$\sqrt{\frac{(d \quad b)E_{c0}}{dbE_1E_2} \ \frac{3G_{12}G_{23}}{bG_{23} \quad dG_{12}}} \ . \tag{9}$$

In Eq. (9), E and G with numerical subscripts denote the Young's and shear moduli of a UD composite lamina (with the subscripts 1 and 2 corresponding to the in-plane fiber and transverse directions, respectively), d is the half-thickness of the transverse plies, and b is the thickness of the outer, constraining 0° plies. (Note that Eq. (9) provides an optimal estimate of the shear-lag parameter, as demonstrated in [22].)

The best-fit estimates of $C_{init} = 0.19$ and $C_{prop} = 0.37$ reported in [14] markedly exceed those derived in Sect. 2. The discrepancy is likely to be caused by the simplified, regular cracking model adopted in Sect. 2. Monitoring of the progressive cracking reveals that the crack spacing distribution evolves during loading [23]. Even in an advanced fragmentation stage, at comparatively large strains, a significant scatter in crack spacing is present [19]. In order to approximately account for the effect of variation in spacings within a deterministic model, the introduction of correction factors is not unusual (see, e.g., [24]). In the following, we will use the best-fit values of C_{init} and C_{prop} determined in [14], in conjunction with the shear-lag parameter given by Eq. (9).

The stress at the onset of crack propagation, $\quad_{prop}$, is related to the mode I intralaminar toughness G_c as

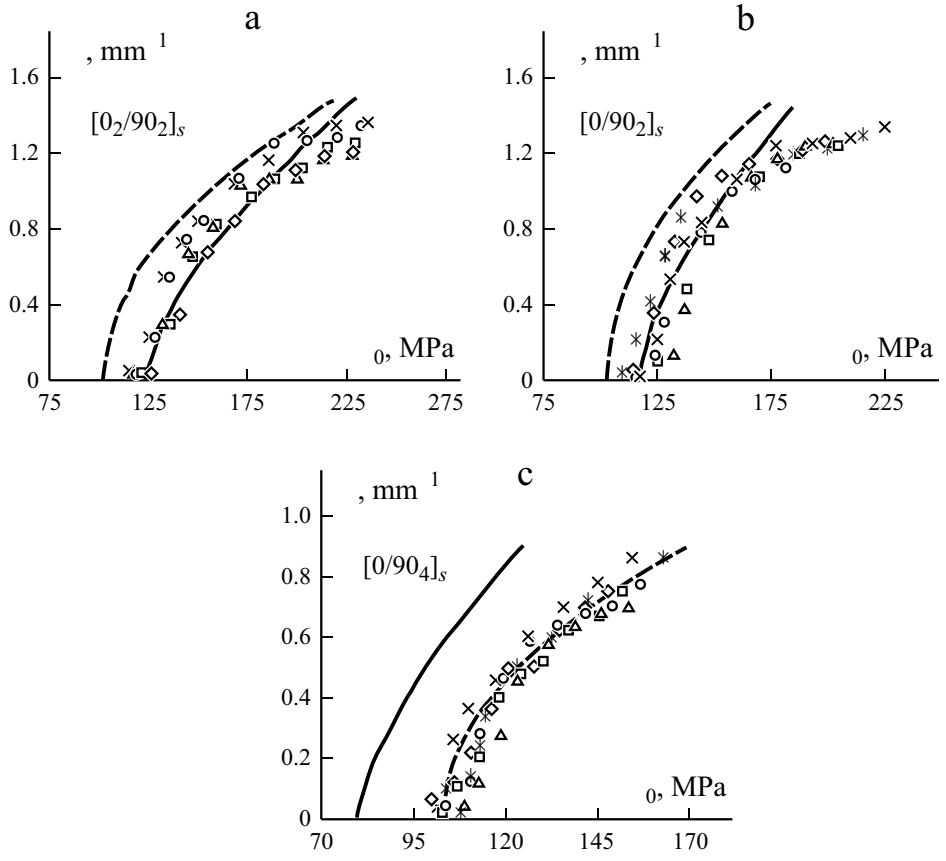

Fig. 2. Crack density as a function of ply stress for $[0_2/90_2]_s$ (a), $[0/90_2]_s$ (b), and $[0/90_4]_s$ (c) laminates. The test results are shown by different markers for each specimen tested; dashed line — Eq. (5) with $_{\text{init}}$ = 103 MPa, solid line — Eq. (8) with $_{\text{prop}}$ given by Eq. (10) and G_{c} 400 J/m^2.

$$_{\text{prop}} \quad \sqrt{\frac{G_{\text{c}} E_2}{2d\,\bar{u}}}, \tag{10}$$

where $\bar{u}$ is the normalized average crack face displacement [6]. Equation (10) is easily derived considering the work of crack closure for estimating the steady-state ERR, which must be equal to G_{c} at the propagation stress. The nondimensional displacement $\bar{u}$ is evaluated by an approximate relation, based on a series of FEM calculations, which has the following form for a crack in the inner transverse layer of a cross-ply composite [6]:

$$\bar{u} \quad A \quad B \left(\frac{E_2}{E_1}\right)^{n} \tag{11}$$

with $A = 0.52$, $B = 0.3075 + 0.1652\dfrac{d \quad b}{b}$, and

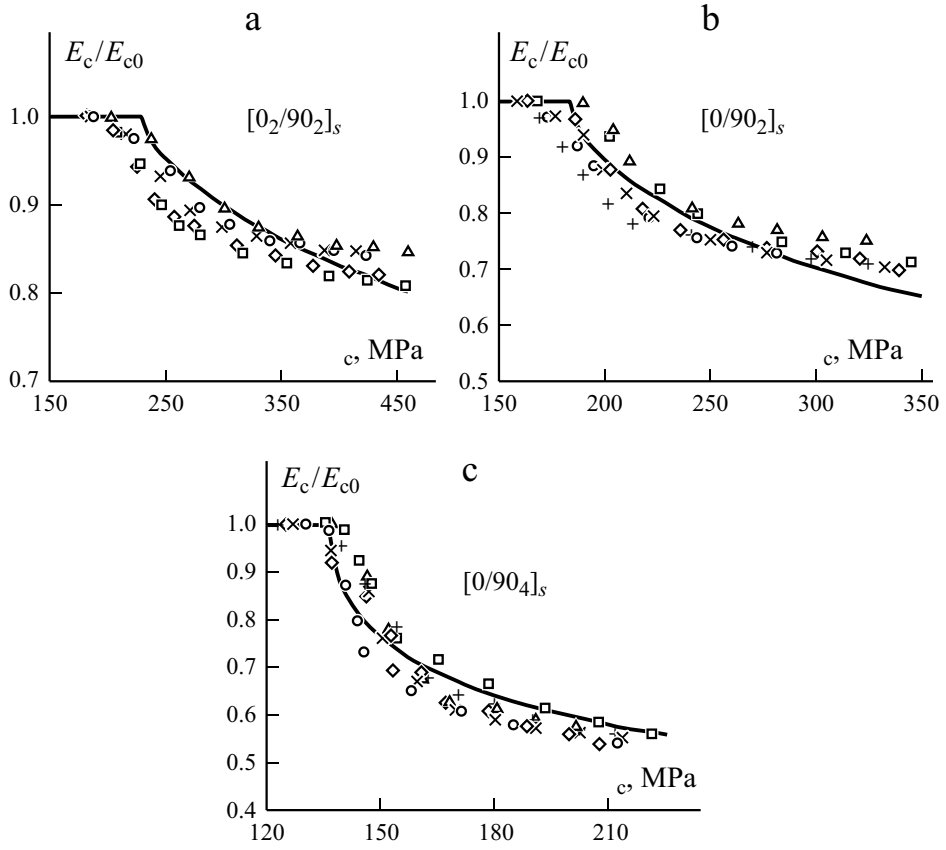

Fig. 3. Young's modulus as a function of applied stress for $[0_2/90_2]_s$ (a), $[0/90_2]_s$ (b), and $[0/90_4]_s$ (c) laminates. Different markers show the results for each specimen tested; the theoretical relation, Eq. (12), is plotted by a solid line.

$$n = 0.030667 \left(\frac{d}{b}\right)^2 - 0.0626 \frac{d}{b} + 0.7037.$$

3.2. Crack density evolution. Consider the cross-ply glass/epoxy laminates with $[0_2/90_2]_s$, $[0/90_2]_s$, and $[0/90_4]_s$ lay-ups studied previously in [19, 25, 26]. A probabilistic cracking model was used in [19], allowing the prediction of crack spacing distribution at high CD. The theoretical spacing distributions agreed nicely with experimental data [19]; however, the account of the scatter in crack locations exerted a marginal effect on the accuracy of the estimated stiffness reduction [19, 25]. In [26], the critical ERR as a function of strain was derived from the measured energy dissipation and data on reduction in the elastic modulus, thus characterizing the statistical distribution of toughness of the transverse ply. It was demonstrated that the evolution of CD with strain could be very accurately predicted by using such a critical ERR dataset.

The increase in the transverse CD in the laminates mentioned is shown in Fig. 2 as a function of the far-field ply stress $_0$. Cracking in the $[0_2/90_2]_s$ laminate, with relatively thin transverse plies and strong constraint due to the thick outer plies, is likely to be propagation-controlled. Taking $_{prop}$ equal to the experimental crack onset stress, the critical ERR is estimated by Eq. (10) at $G_c = 400$ J/m^2. Using this G_c value, $_{prop}$ for the other two lay-ups was determined by Eq. (10), and the theoretical

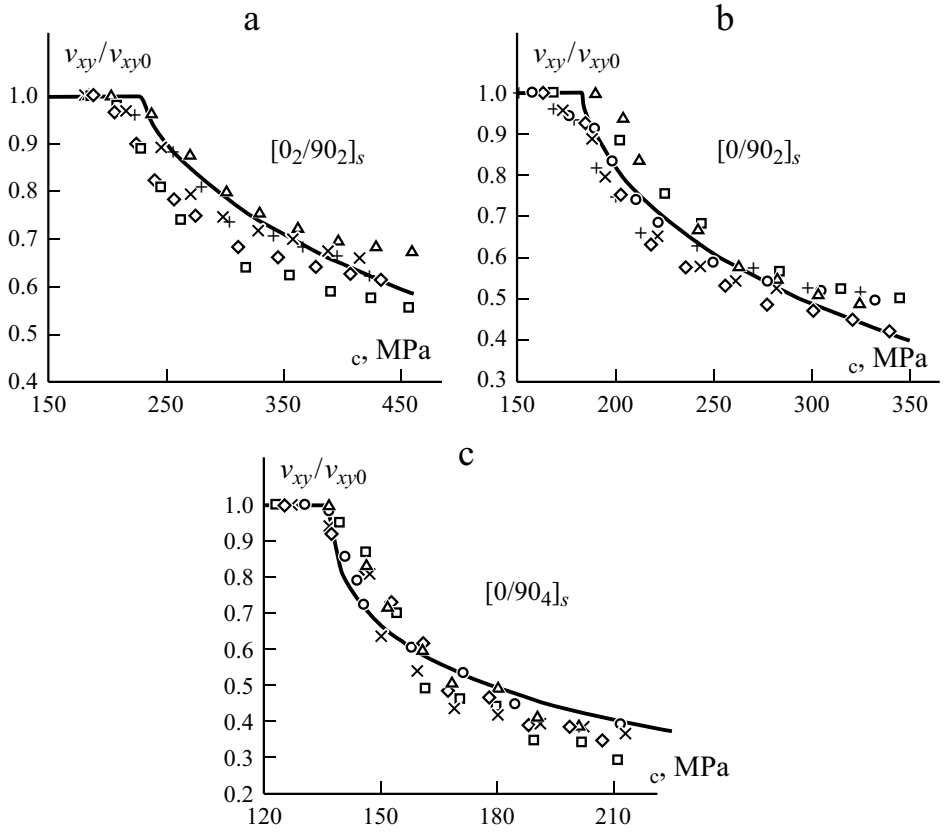

Fig. 4. Poisson's ratio as a function of applied stress for $[0_2/90_2]_s$ (a), $[0/90_2]_s$ (b), and $[0/90_4]_s$ (c) laminates. Different markers show the results for each specimen tested; the theoretical relation, Eq. (13), is plotted by a solid line.

CD diagrams for propagation-controlled cracking according to Eq. (8) were plotted by solid lines in Fig. 2. A reasonable agreement with experimental CD data for the laminates with thinner transverse plies is seen (Fig. 2a,

b). For twice thicker transverse plies, $_{\text{prop}}$ markedly underestimates the crack onset stress (Fig. 2c). This suggests that the cracking is initiation-controlled, and $_{\text{init}}$ = 103 MPa is determined as the crack onset stress in the $[0/90_4]_s$ laminate. The initiation-controlled cracking diagrams given by Eq. (5) are shown in Fig. 2 by dashed lines.

There is a close correspondence between the interplay of initiation and propagation criteria as applied to crack onset (Fig. 1) and progressive cracking (Fig. 2). In both cases, initiation governs the cracking of cross-ply laminates with thick transverse plies, while propagation dominates in thin plies. Namely, for thin transverse plies, the crack initiation stress is reached first, and the load has to be increased to meet the propagation criterion. Likewise, considering a fixed crack density, the initiation criterion is fulfilled at a lower stress than the propagation criterion for the $[0_2/90_2]_s$, and $[0/90_2]_s$ laminates. The opposite sequence holds for thick transverse plies (Fig. 2c). Although the overall agreement between the theoretical relations and test results in Fig. 2 is inferior to that reached in [26], only two parameters characterizing crack resistance of the material, $_{\text{init}}$ and G_c, are needed, as opposed to the exhaustive characterization of G_c distribution performed in [26].

At high stresses, the CD diagram determined by Eq. (5) tends to overtake that given by Eq. (8), as seen in Fig. 2a, b. This can be interpreted as a change in the cracking mechanism of the laminates from a propagation-controlled to an initia-

tion-controlled one during loading. Such a transition naturally follows from the flaw-based model of transverse cracking [12]. Initially, a laminate may contain a population of flaws with a wide size distribution. The presence of relatively large microcracks, with dimensions comparable to the thickness of the transverse ply, ensures that their propagation controls cracking. During loading accompanied by progressive cracking, the large-size part of the population of flaws is exhausted, leaving only small-size flaws, and the transverse ply becomes effectively thick [12], with prevalent initiation-controlled cracking.

3.3. Stiffness reduction. We proceed by estimating the reduction in the elastic modulus and Poisson's ratio of the laminates as a function of applied stress, by using the respective master curves for CD. The testing procedure and results have been detailed elsewhere [19, 25]. Subsequent loading-unloading cycles with increasing maximum stress were applied to the laminates, and the relevant mechanical characteristics were determined after each cycle. The evolution of the laminate characteristics with the maximum stress sustained is shown in Figs. 3 and 4. The normalizing parameters E_{c0} and $_{xy0}$ here and in [25] correspond to the last loading cycle immediately preceding the onset of cracking.

We apply the closed-form expressions of the effective in-plane thermomechanical constants of a cracked laminate derived in [6] in terms of the thermoelastic properties of the plies, their lay-up, and CD. For cross-ply laminates containing cracks only in the transverse ply, located in the middle of the laminate, the following relations hold:

$$\frac{E_c}{E_{c0}} \quad \frac{1}{1 \quad \frac{E_2}{1 \quad _{12} \quad _{21}}(1 \quad _{12} \quad _{xy0})g_3 k \quad _n \bar{u}}, \tag{12}$$

$$\frac{_{xy}}{_{xy0}} \quad \frac{1 \quad \frac{E_2}{1 \quad _{12} \quad _{21}} \quad \frac{_{12} \quad _{yx0}}{_{yx0}} g_3 k \quad _n \bar{u}}{1 \quad \frac{E_2}{1 \quad _{12} \quad _{21}}(1 \quad _{12} \quad _{xy0})g_3 k \quad _n \bar{u}}, \tag{13}$$

where the quantities with the subscript 0 relate to an intact laminate, the numerical subscripts of the mechanical parameters imply the properties of the UD composite, and the remaining parameters are

$$g_3 \quad \frac{d}{E_1 b} \quad ^2_{12} \frac{b \quad d}{\frac{E_1}{E_2} d \quad b} \quad 1 \;, \quad \frac{1}{k} \quad \frac{E_2 d}{2E_1 b} \quad 1 \quad \frac{E_1 b}{E_2 d} \quad \frac{^2_{12}(b \quad d)^2}{d \quad \frac{E_1}{E_2} d \quad b} \;.$$

The nondimensional transverse CD, designated by $_n$, is obtained as $_n \quad 2d$, and $\bar{u}$ is evaluated by Eq. (11).

According to the results of cracking analysis in Sect. 3.2, the CD as a function of applied stress in Eqs. (12) and (13) is determined by Eq. (5) for the $[0/90_4]_s$ laminate and by Eq. (8) for the $[0_2/90_2]_s$ and $[0/90_2]_s$ laminates, by using Eq. (1) to link the applied stress and the ply stress. It is seen that the reduction in the Young's modulus of laminates predicted by Eq. (12) (Fig. 3) and in Poisson's ratio predicted by Eq. (13) (Fig. 4) are in a reasonably good agreement with test results, although somewhat inferior to that obtained by using the experimental CD as an input for the stiffness model [25].

4. Conclusions

Master-curve equations for the crack density as a function of ply stress, complying with a deterministic failure criterion, are derived. Different analytical expressions for the criteria of strength and critical energy release rate, corresponding to the initiation-controlled and propagation-controlled cracking mechanisms, are obtained. By analyzing the progressive cracking diagrams of GFRP cross-ply composite laminates, it is shown that both the initiation and the propagation conditions are met at cracking, and the experimental crack density data follow a master curve consistent with the predominant cracking mechanism. The cracking master curves are also successfully applied to modeling the laminate stiffness reduction.

Acknowledgments. E. Spārniņš gratefully acknowledges the support by the ESF.

REFERENCES

1. J. A. Nairn, "Matrix microcracking in composites," in: A. Kelly and C. Zweben (eds.), Comprehensive Composite Materials. Vol. 2, Pergamon (2000), pp. 403-432.
2. M. Yu. Kashtalyan and C. Soutis, "Mechanisms of internal damage and their effect on the behavior and properties of cross-ply composite laminates," Int. Appl. Mech., **38**, 641-657 (2002).
3. J.-M. Berthelot, "Transverse cracking and delamination in cross-ply glass-fiber and carbon-fiber reinforced plastic laminates: static and fatigue loading," Appl. Mech. Rev., **56**, 111-147 (2003).
4. M. Kashtalyan and C. Soutis, "Analysis of composite laminates with intra- and interlaminar damage," Progr. Aerosp. Sci., **41**, 152-173 (2005).
5. R. Joffe and J. Varna, "Analytical modeling of stiffness reduction in symmetric and balanced laminates due to cracks in 90 layers," Compos. Sci. Technol., **59**, 1641-1652 (1999).
6. P. Lundmark and J. Varna, "Constitutive relationships for laminates with ply cracks in in-plane loading," Int. J. Damage Mech., **14**, 235-259 (2005).
7. K. Garrett and J. Bailey, "Multiple transverse fracture in 90 cross-ply laminates of a glass fibre–reinforced polyester," J. Mater. Sci., **12**, 157-168 (1977).
8. K. Garrett and J. Bailey, "The effect of resin failure strain on the tensile properties of glass fibre–reinforced polyester cross-ply laminates," J. Mater. Sci., **12**, 2189-2194 (1977).
9. A. Parvizi, K. Garrett, and J. Bailey, "Constrained cracking in glass fibre-reinforced epoxy cross-ply laminates," J. Mater. Sci., **13**, 195-201 (1978).
10. A. Parvizi and J. Bailey, "On multiple transverse cracking in glass fiber epoxy cross-ply laminates," J. Mater. Sci., **13**, 2131-2136 (1978).
11. V. V. Vasil'ev, A. A. Dudchenko, and A. N. Elpat'evskii, "Analysis of the tensile deformation of glass-reinforced plastics," Polym. Mech., **6**, 127-130 (1970).
12. G. J. Dvorak and N. Laws, "Analysis of progressive matrix cracking in composite laminates II. First ply failure," J. Compos. Mater., **21**, 309-329 (1987).
13. S. Abe, K. Kageyama, I. Ohsawa, M. Kanai, and T. Kato, "Analytical prediction and experiment of transverse lamina cracking in multidirectionally reinforced symmetric laminates," in: Proc. of 7th Japan Int. SAMPE Symp. and Exhibit. (2001), pp. 817-820.
14. J. Andersons, R. Joffe, E. Spārniņš, and O. Rubenis, "Progressive cracking mastercurves of the transverse ply in a laminate," Polym. Compos. (in press).
15. J. Bailey and A. Parvizi, "On fiber debonding effects and the mechanism of transverse-ply failure in cross-ply laminates of glass fibre/thermoset composites," J. Mater. Sci., **16**, 649-659 (1981).
16. L. Boniface, P. A. Smith, M. G. Bader, and A. H. Rezaifard, "Transverse ply cracking in cross-ply CFRP laminates — initiation or propagation controlled?" J. Compos. Mater., **31**, 1080-1112 (1997).
17. P. Gudmundson and J. Alpman, "Initiation and growth criteria for transverse matrix cracks in composite laminates," Compos. Sci. Technol., **60**, 185-195 (2000).
18. P. Ladeveze, G. Lubineau, and D. Violeau, "A computational damage micromodel of laminated composites," Int. J. Fract., **137**, 139-150 (2006).
19. J. Andersons, R. Joffe, and E. Spārniņš, "Statistical model of the transverse ply cracking in cross-ply laminates by strength and fracture toughness based failure criteria," Eng. Fract. Mech., **75**, 2651-2665 (2008).
20. N. Laws and G. J. Dvorak, "Progressive transverse cracking in composite laminates," J. Compos. Mater., **22**, 900-916 (1988).

21. J. W. Lee and I. M. Daniel, “Progressive transverse cracking of cross-ply composite laminates,” J. Compos. Mater., **24**, 1225-1243 (1990).
22. J. A. Nairn and D. A. Mendels, “On the use of planar shear-lag methods for stress-transfer analysis of multilayered composites,” Mech. Mater., **33**, 335-362 (2001).
23. P. W. Manders, T.-W. Chou, F. R. Jones, and J. W. Rock, “Statistical analysis of multiple fracture in 0 /90 /0 glass fibre/epoxy resin laminates,” J. Mater. Sci., **18**, 2876-2889 (1983).
24. S. Liu and J. A. Nairn, “The formation and propagation of matrix microcracks in cross-ply laminates during static loading,” J. Reinf. Plast. Compos., **11**, 158-178 (1992).
25. O. Rubenis, E. Spārniņš, J. Andersons, and R. Joffe, “The effect of crack spacing distribution on stiffness reduction of cross-ply laminates,” Appl. Compos. Mater., **14**, 59-66 (2007).
26. D. T. G. Katerelos, J. Varna, and C. Galiotis, “Energy criterion for modelling damage evolution in cross-ply composite laminates,” Compos. Sci. Technol., **68,** 2318-2324 (2008).